

# Investigation of the reaction product of 1,4,7,10-tetraphenyl-cyclododecahexa-1,2,3,7,8,9-ene with dodecacarbonyl-triiron by X-ray diffraction and MS: comparative structural study of the hexacarbonyl- $\mu_2$ -(1 $\eta^2$ -1,2-ene-2 $\eta^3$ -3,4,5-allyl-1 $\sigma^1$ -5)diiron(Fe–Fe) system

Andrzej Zimniak <sup>a,\*</sup>, Janusz Zachara <sup>b</sup>, Marian Olejnik <sup>c</sup>

<sup>a</sup> Faculty of Pharmacy, Medical University of Warsaw, 02-097 Warsaw, Poland

<sup>b</sup> Department of Chemistry, Warsaw University of Technology, 00-664 Warsaw, Poland

<sup>c</sup> Institute of Organic Chemistry, Polish Academy of Sciences, 01-224 Warsaw, Poland

Received 12 May 1999; received in revised form 14 July 1999

## Abstract

Reaction of dodecacarbonyl-triiron with the 12-membered bis(butatriene) results in phenyl ring metallation and an intramolecular crosslinking of the macrocycle with the formation of a system of three condensed rings. The central core of the complex is formed by  $\text{Fe}_2(\text{CO})_6$  unit bridged by an organic ligand which is  $\eta^3$ : $\eta^1$ -bonded by the  $\pi$ -allylic system and  $\eta^2$ -bonded by the olefinic group. The molecular structure of the complex was determined by X-ray diffraction. Differences in fragmentation patterns in MS (EI and LSIMS) were examined. Comparative studies of the geometry of the complex obtained and a series of compounds with isostructural core have been carried out. © 1999 Elsevier Science S.A. All rights reserved.

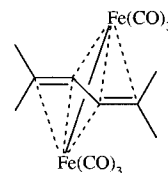
**Keywords:** Iron complex; Crystal structure; Mass spectra; Bis(tricarbonyl iron); Macrocylic bis(butatriene)

## 1. Introduction

In reaction of dodecacarbonyl-triiron with the single butatriene system, complexes containing binuclear  $[\text{Fe}(\text{CO})_3]_2$  core attached to the ligand with two identical asymmetric allylic  $\pi$  bonds [1–6] are formed (Scheme 1). In arene-substituted derivatives of butatriene, the aromatic rings are not involved in the complexation.

During the investigations of the complexation reac-

tions of bis-cumulene 12-membered macrocyclic system with iron carbonyls, several organocarbonyliron compounds have been obtained [7]. In the reaction with  $\text{Fe}_3(\text{CO})_{12}$ , a product of the composition  $[\text{L}\cdot\text{Fe}_2(\text{CO})_6]$  was isolated in two isomeric forms. This composition could suggest the engagement in the complexation of only one of the cumulene chains but this was contradicted by the analysis of the UV spectra — the strong



Scheme 1. Schematic structure of complexes obtained from a butatriene system in reaction with  $\text{Fe}_3(\text{CO})_{12}$ .

**Abbreviations:** L, organic ligand of the complex **I**; MS, mass spectrometry; EI, electron impact; LSIMS, liquid secondary ion mass spectrometry; NBA, *m*-nitrobenzyl alcohol; MIKE, mass-analyzed ion kinetic energy; PFK, perfluorokerosene; PFTBA, hepta-cosafluorotributylamine.

\* Corresponding author. Fax: +48-22-8231487.

E-mail address: axzimni@farm.amwaw.edu.pl (A. Zimniak)

maximum at  $\lambda = 366$  nm typical for this butatriene system was absent. Therefore, the structure of the new complex was completely different from the known symmetric double  $\pi$ -allyl system.

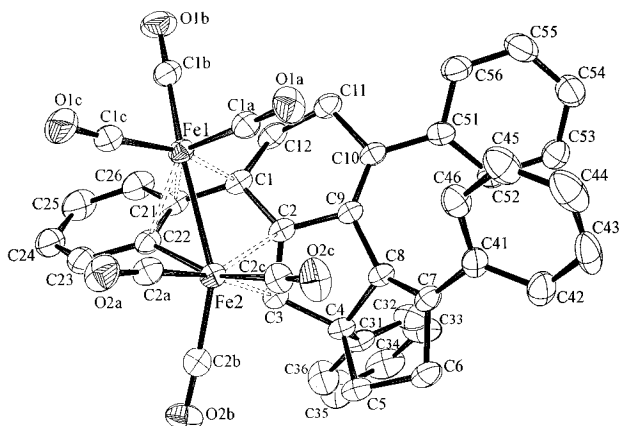


Fig. 1. ORTEP diagram of **I** on 30% probability level showing the atom labeling scheme. Hydrogen atoms are omitted for clarity.

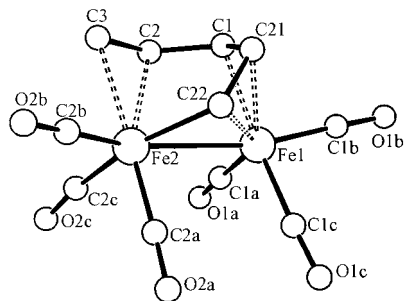


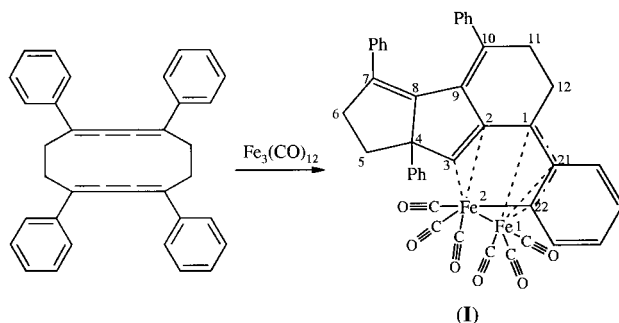
Fig. 2. General view of the central core structure in complexes investigated.

## 2. Results and discussion

Of the two isomeric complexes obtained in the reaction of cyclic (bis)butatriene system with dodecacarbonyl-triiron (Scheme 2), only one isomer (**I**) formed well-shaped crystals suitable for X-ray analysis. The other isomer was isolated with a very low yield (ca. 1%).

### 2.1. Molecular structure

As found by X-ray crystallographic studies, reaction with dodecacarbonyl-triiron causes a dramatic structural rearrangement in the molecule of the macrocyclic bis(butatriene), resulting in intramolecular crosslinking of the cumulene chains and in forming three condensed rings: two five- and one six-membered. Furthermore, migration of the hydrogen atom from



Scheme 2. Complexation reaction of tetraphenyl-bis(butatriene) with  $\text{Fe}_3(\text{CO})_{12}$ .

position C(22) in the phenyl ring to the carbon C(3) of the former cumulene chain occurred, followed by metallation of this ring by the iron atom. The molecular structure of the complex is shown in Fig. 1. Selected bond lengths and bond angles are presented in Table 1.

The central core of the complex, as shown in Fig. 2, is formed by two  $\sigma$ -bonded  $\text{Fe}(\text{CO})_3$  units, linked to the organic ligand so that Fe(1) is  $\eta^3$ -bonded to the allylic system including the carbon atoms C(1)C(21)C(22), whereas Fe(2) is  $\eta^2$ -bonded to olefinic carbons C(2):C(3) and  $\sigma$ -bonded to C(22). The carbon atom

Table 1  
Selected bond lengths (Å), valence and torsion angles (°) for **I**

Bond lengths (Å)			
Fe(1)–C(1A)	1.768(3)	Fe(2)–C(2A)	1.761(3)
Fe(1)–C(1B)	1.787(3)	Fe(2)–C(2B)	1.778(3)
Fe(1)–C(1C)	1.812(3)	Fe(2)–C(2C)	1.836(3)
Fe(1)–C(1)	2.081(2)	Fe(2)–C(22)	2.005(2)
Fe(1)–C(21)	2.122(2)	Fe(2)–C(3)	2.202(2)
Fe(1)–C(22)	2.126(2)	Fe(2)–C(2)	2.335(2)
Fe(1)–Fe(2)	2.6305(8)	C(1)–C(21)	1.438(3)
C(1)–C(2)	1.455(3)	C(1)–C(12)	1.501(3)
C(2)–C(3)	1.397(3)	(2)–C(9)	1.491(3)
C(3)–C(4)	1.531(3)	C(9)–C(10)	1.351(3)
C(21)–C(22)	1.426(3)	C(21)–C(26)	1.430(3)
C(22)–C(23)	1.429(4)	C(23)–C(24)	1.357(4)
C(24)–C(25)	1.401(5)	C(25)–C(26)	1.354(4)
Bond angles (°)			
C(1)–Fe(1)–C(21)	40.01(9)	C(22)–Fe(2)–C(3)	87.24(9)
C(1)–Fe(1)–C(22)	69.60(10)	C(22)–Fe(2)–C(2)	80.02(9)
C(21)–Fe(1)–C(22)	39.24(10)	C(3)–Fe(2)–C(2)	35.72(8)
O(1A)–C(1A)–Fe(1)	177.8(2)	O(2A)–C(2A)–Fe(2)	175.1(2)
O(1B)–C(1B)–Fe(1)	178.2(2)	O(2B)–C(2B)–Fe(2)	176.9(2)
O(1C)–C(1C)–Fe(1)	176.1(3)	O(2C)–C(2C)–Fe(2)	171.9(2)
C(21)–C(1)–C(2)	115.3(2)	C(3)–C(2)–C(1)	126.8(2)
C(3)–C(2)–C(9)	110.4(2)	C(1)–C(2)–C(9)	119.8(2)
C(10)–C(9)–C(2)	121.4(2)	C(22)–C(21)–C(1)	113.9(2)
C(1C)–Fe(1)–Fe(2)	–4.72(12)	C(1A)–Fe(1)–Fe(2)	5.52(11)
–C(2A)		–C(2C)	
C(21)–C(1)–C(2)–C(3)	23.9(3)	C(1)–C(2)–C(3)–C(4)	157.3(2)
C(2)–C(1)–C(21)–C(22)	42.2(3)	C(1)–C(21)–C(22)	–12.5(3)
		–Fe(2)	

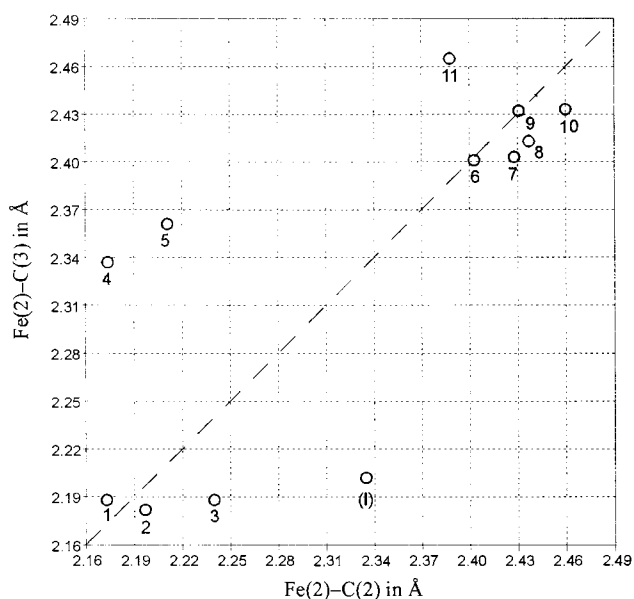


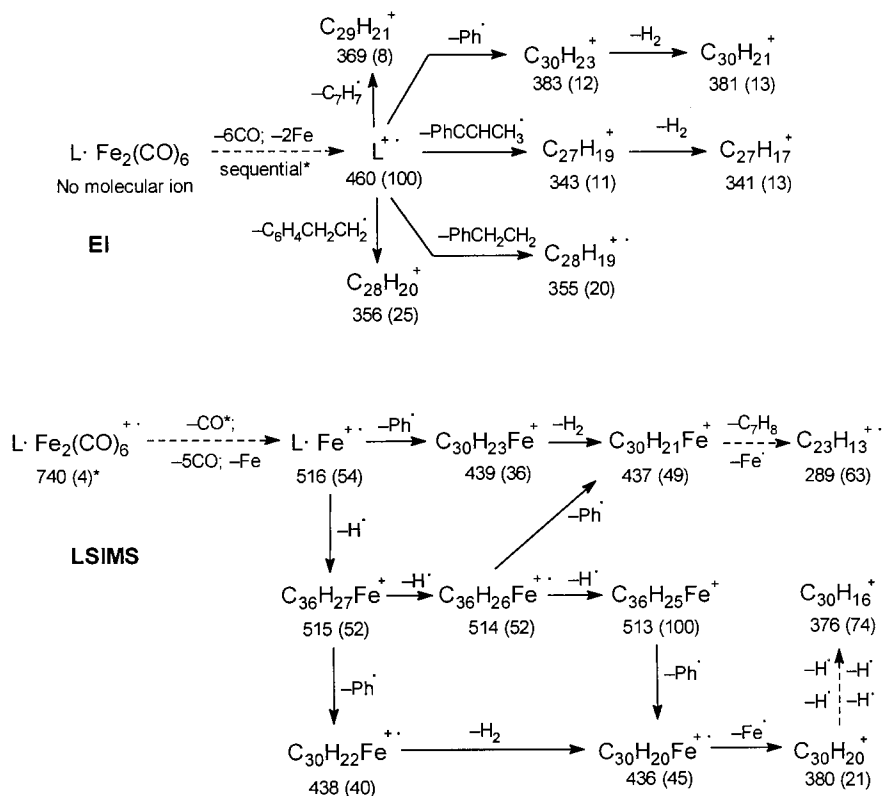
Fig. 3. Scatter plot of Fe(2)–C(2) vs. Fe(2)–C(3) bond lengths in (Å) observed in complexes **I–III** and **I**.

C(1) is located near the mean plane of the metallated ring C(21)–C(26) (deviation 0.083(4) Å) while the deviation of Fe(2) atom is 0.279(4) Å. The  $\pi$ -allylic bond

Fe(1)–C(1)C(21)C(22) is almost symmetric, the bond lengths being: Fe(1)–C(1) 2.081(2), Fe(1)–C(21) 2.122(2) and Fe(1)–C(22) 2.126(2) Å. The important feature of this structure is that Fe(2) is asymmetrically bonded to the olefinic part of the molecule, C(2):C(3). The respective distances are: Fe(2)–C(2) 2.335(2), Fe(2)–C(3) 2.202(2) Å.

The bond system observed in the central core of the complex **I** is found in a series of structurally characterized compounds taken from the Cambridge Structural Database (CSD) [8] (11 entries [9–19]). The general folding of the central core in these complexes is in agreement with that observed in **I**. Selected structural data for **I** and for compounds chosen from the CSD are collected in Table 2. Thus, the Fe(1)–Fe(2) bond length in **I** is 2.6305(8) Å and corresponds well with the mean value of 2.629 Å calculated for above-mentioned 11 structures (maximum and minimum values are 2.667 and 2.602 Å). For comparison, the bond length between iron atoms in Fe<sub>2</sub>(CO)<sub>9</sub> is 2.523 Å [20], and in the symmetric bis( $\pi$ -allylic) complex with a binuclear [Fe(CO)<sub>3</sub>]<sub>2</sub> central core obtained from butatriene, it is 2.591 Å [3].

The above group of complexes can be divided into two sets that differ in the length of the  $\pi$ -bond, ex-



Scheme 3. Proposed EI and LSIMS mass spectral fragmentation pattern for **I**, where L means the organic ligand C<sub>36</sub>H<sub>28</sub>. Under formulas of ions the *m/z* values are presented (relative intensities of signals in brackets). Composition of fragments marked by asterisks was not confirmed by accurate mass measurements because of low intensity of their signals.

pressed as a mean value of the interatomic distances Fe(2)–C(2) and Fe(2)–C(3), for which high values of standard deviation were observed. As expected, the  $\pi$ -bond is significantly weaker in the case of aromatic donor (mean length 2.425 Å) as compared with the olefinic one (2.232 Å). The differences in  $\pi$ -bond are outlined in Fig. 3 (complexes **8–11**, **1–5**, and **I**, respectively; see also mean values of the  $\pi$ -bonds in Table 2).

In general, the  $\pi$ -bond is nearly symmetric except for compounds in which the donor is unilaterally conjugated, e.g. in compounds **4** and **5** (Table 2). In these complexes the carbon atom C(3) is bound to the alkoxy group, and the distance Fe(2)–C(3) is longer by 0.163 and 0.150 Å, respectively, as compared with Fe(2)–C(2). A similar asymmetry was observed in **11** with an ester moiety at C(3) carbon atom, in which the Fe(2)–C(3) distance is longer by 0.077 Å than that between Fe(2) and C(2) atoms.

In contrast to the increased Fe(2)–C(3) distance in the compounds described above, in complex **I** the Fe(2)–C(2) bond is weaker, i.e. longer by 0.133 Å. This can be explained by the coupling with the olefinic moiety C(9)–C(10), which is bound to the other side of the  $\pi$ -donor (to the atom C(2), see Fig. 3).

The lability of  $\pi$ -bonding expressing itself in substantial changes of bond lengths and deviations from symmetry within the group of compared compounds is critical for conformation of the chain C(22)C(21)–

C(1)C(2)C(3), containing both  $\pi$  and  $\pi$ -allylic donor systems. Thus, significant correlations between the absolute value of the torsion angle C(22)–C(21)–C(1)–C(2) and the length of the Fe(2)–C(3) bond (correlation coefficient  $R = 0.821$ ), as well as the C(21)–C(1)–C(2)–C(3) angle and the Fe(2)–C(2) distance (correlation coefficient  $R = -0.812$ ) have been observed.

For the complexes under study, the conformation of terminal carbonyl groups in the central [Fe(CO)<sub>3</sub>]<sub>2</sub> core is close to *syn*-periplanar (the values of torsion angles C(1c)–Fe(1)–Fe(2)–C(2a) and C(1a)–Fe(1)–Fe(2)–C(2c) are given in Table 2). The lowest deviations from the theoretical *syn*-periplanar conformation were noted for the compound **I**.

## 2.2. Mass spectral investigations

As observed earlier [4], for complexes obtained from a single butatriene system, having binuclear structure [L·Fe(CO)<sub>3</sub>]<sub>2</sub> with the core attached to the ligand (L) with two identical asymmetric allylic  $\pi$ -bonds, the fragmentation pattern starts with successive loss of six CO groups and both iron atoms. In contrast to that, in complexes formed from phenyl-substituted aldazines only the CO groups are split off prior to fragmentation of the ligand, which begins in the [L·Fe<sub>2</sub>]<sup>+</sup> moiety [21]. This is presumably due to the strong  $\sigma$ -bonds between

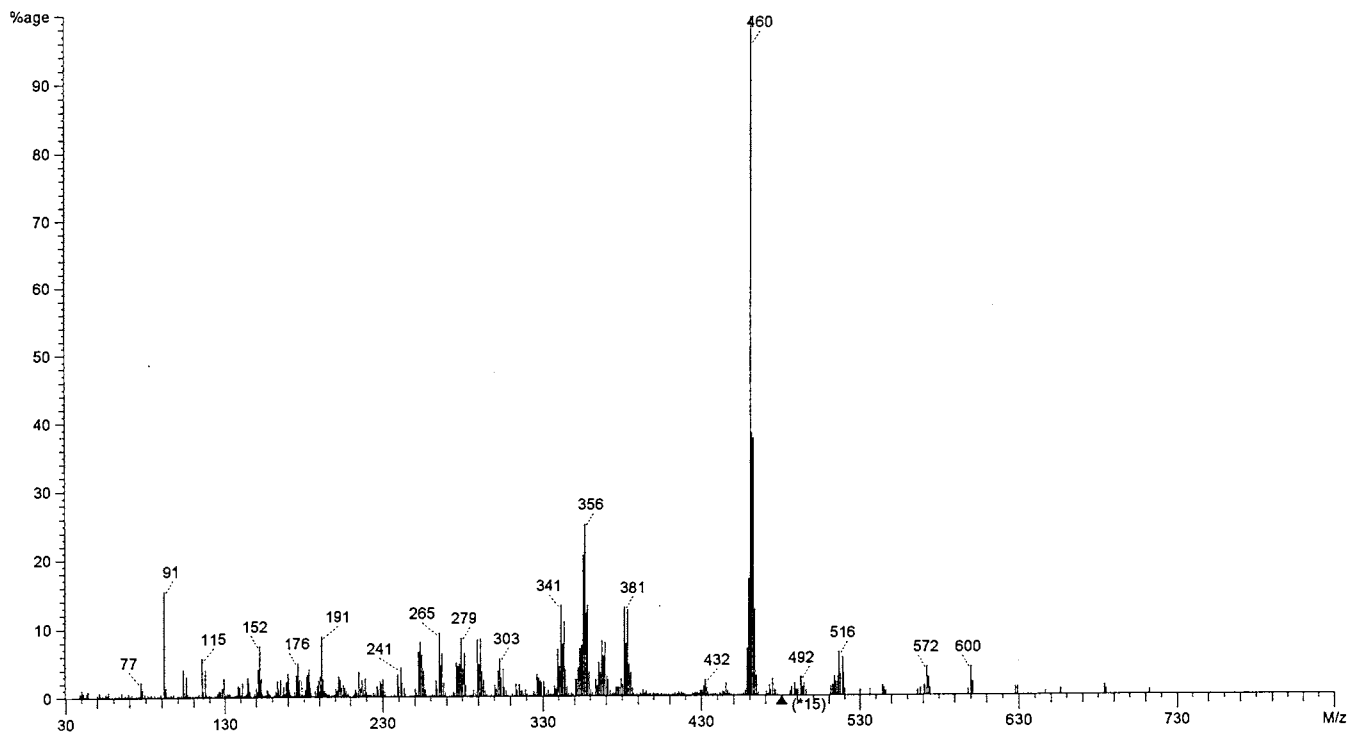


Fig. 4. EI mass spectrum of **I**.

Table 2  
Selected structural data, distances in (Å) and torsion angles in (°), for compared complexes I–II and for I

	Fe–Fe	Fe(2)–C(3)	Fe(2)–C(2)	$\pi$ -bond <sup>a</sup>	C(2)–C(3)	Fe(1)–C(1)	Fe(1)–C(21)	Fe(1)–C(22)	C(1)–C(21)	C(21)–C(22)	Fe(2)–C(22)	T <sub>1</sub> <sup>b</sup>	T <sub>2</sub> <sup>b</sup>	References
SACJEL	1	2.613	2.188	2.181	1.388	2.139	2.073	2.027	1.430	1.419	1.993	12.1	–2.0	[9]
KAVPOM	2	2.667	2.182	2.190	1.383	2.032	2.059	2.333	1.421	1.433	1.997	26.1	3.6	[10]
HCXOFE	3	2.642	2.188	2.214	1.399	2.080	2.077	2.088	1.412	1.404	2.002	14.4	1.8	[11]
FOJTED	4	2.624	2.337	2.256	1.432	2.084	2.054	2.058	1.450	1.415	2.061	–25.4	–12.2	[12]
CORWEL10	5	2.617	2.361	2.286	1.459	2.093	2.040	2.013	1.431	1.399	2.018	–16.9	–4.6	[13]
HCPAFE	6	2.602	2.401	2.402	1.397	2.084	2.080	2.080	1.443	1.414	1.997	–11.3	–3.4	[14]
JUZLIZ	7	2.645	2.403	2.416	1.402	2.123	2.066	2.055	1.429	1.393	1.957	–14.8	–0.6	[15]
KETFEB11	8	2.624	2.413	2.425	1.403	2.067	2.105	2.122	1.442	1.436	1.985	–13.7	–2.8	[16]
CEDZIU	9	2.635	2.432	2.432	1.392	2.068	2.084	2.129	1.440	1.415	1.969	–24.1	–8.7	[17]
KETFEB	10	2.629	2.433	2.447	1.398	2.072	2.110	2.119	1.424	1.434	1.991	–13.9	–3.2	[18]
BIFXOD	11	2.621	2.465	2.427	1.414	2.102	2.077	2.071	1.435	1.429	1.986	10.7	1.1	[19]
(I)		2.631	2.202	2.269	1.397	2.081	2.122	2.126	1.438	1.426	2.005	4.7	–5.5	
SD sample		0.017	0.111	0.105	0.021	0.028	0.024	0.082	0.011	0.014	0.026			
Mean		2.629	2.334	2.328	1.405	2.085	2.079	2.102	1.433	1.418	1.997			

<sup>a</sup> The length of the  $\pi$ -bond is given as a mean value of distances Fe(2)–C(2) and Fe(2)–C(3).

<sup>b</sup> T<sub>1</sub> and T<sub>2</sub> mean following the torsion angles: C(1e)–Fe(1)–Fe(2)–C(2a) and =C(1a)–Fe(1)–Fe(2)–C(2c), respectively.

the iron and nitrogen atoms and also metallation of the aromatic ring in complexes obtained from phenylaldazines [22]. The MS measurements described in Refs. [4,21] were carried out using EI ionization.

In the present work two distinct fragmentations for complex I have been noted (shown in Scheme 3), depending on whether the EI or LSIMS method was applied.

### 2.2.1. EI method

When the classic EI ionization method was applied, no molecular ion has been observed and the first very weak signal occurred at  $m/z$  712 (intensity 3%) as a consequence of loss of one CO molecule (Fig. 3). A successive loss of the next five CO moieties and both Fe atoms results in fragmentation ion at  $m/z$  460 (100%, ca. four times more abundant than the next most intense signal at  $m/z$  356), which represents the ligand C<sub>36</sub>H<sub>28</sub>. EI and LSIMS fragmentation patterns are shown in Scheme 3.

Further fragmentation proceeds along five main pathways, all starting with the ion of the ligand. In general, high mobility of hydrogen atoms could be noted in both EI as well in LSIMS experiments. Phenylethylene molecule is formed, presumably in the rearrangement of the phenyl substituent. Alternatively, an independent loss in one step of the phenyl group and of the ethylene molecule could be considered. An analogous loss of the C<sub>6</sub>H<sub>4</sub> ring (phenyl initially dehydrogenated by metallation in complexation reaction) with ethylene results in the ion at  $m/z$  356. Without rearrangement of the phenyl group the phenylpropylene molecule PhC:CHCH<sub>3</sub> can be split off, giving the fragmentation ion at  $m/z$  343. In another pathway, the loss of tolyl group C<sub>7</sub>H<sub>7</sub> was observed. The EI spectrum is shown in Fig. 4.

The described fragmentation of the ion at  $m/z$  460 arising from the ligand was confirmed by the measurements of the metastable ion spectra —B/E linked scan spectrum in the first field-free region and mass-analyzed ion kinetic energy spectrum (MIKE) (daughter ions at  $m/z$  383, 369, 356, 355 and 343; see Fig. 5).

### 2.2.2. LSIMS method

The atypically abundant fragmentation observed in the LSIMS experiment (for spectrum see Fig. 6) correlated with a relatively low intensity of the molecular ion signal points to the lability of the molecule I. Moreover, the fragmentation is significantly different from that obtained by the EI method (Fig. 4). A weak signal (4%) originating from unprotonated molecular ion at  $m/z$  740<sup>1</sup> was followed by loss of six terminal carbonyls and one iron atom. The loss of CO, 3CO, 4CO, 5CO, 6CO and Fe(CO)<sub>5</sub> was noticed, giving fragmentation ions at 712\*, 656, 628, 600, 572, and 544  $m/z$ . The last

CO group split off, resulting in the ion  $[L\cdot Fe]^{+\bullet}$  at  $m/z$  516. In contrast to the EI spectrum, the fragmentation of the organic ligand started in  $[L\cdot Fe]^{+\bullet}$  so that no ion at  $m/z$  460 derived solely from the ligand could be observed.

The spectrum reveals possible loss of toluene with simultaneous removal of the iron atom ( $m/z$  289). Formation of the toluene molecule requires an initial rearrangement of phenyl and hydrogen atoms. Remaining paths of the fragmentation are shown in Scheme 3, one of them leading to the highly unsaturated ion  $C_{30}H_{16}^+$ .

The composition of fragmentation ions discussed above and shown in Scheme 3, investigated by both EI and LSIMS methods, was confirmed by accurate mass measurements (see legend to Scheme 3 for detailed explanation). In the LSIMS experiments, the metastable ions were not measured because of low intensity of signals.

The results of mass spectral investigations of **I** indicate a relatively strong bond between the iron atom and the ligand in  $[L\cdot Fe]^{+\bullet}$ , considering the low stability of the whole molecule. One might assume that the iron atom remains attached to the metallated phenyl ring, since no loss of the  $C_6H_4$  moiety was noted in LSIMS measurements in contrast to the EI method. Furthermore, the abundant signal of the ligand-derived ion ( $m/z$  460) in the EI spectrum testifies to the stability of this group. The above results prove the need to apply both EI and LSIMS techniques to gain complementary results in the MS study of this class of compounds.

### 2.3. Conclusions

The comparison of the structural features of the complexes under study leads to the conclusion that the geometry of the central core is closely correlated with the character of the  $\pi$ -bond. As expected, the strength of this bond is noticeably different for aromatic and olefinic donors. Furthermore, its deviation from symmetry is due to the electronic properties of its substituents conjugated with the donor. The  $\pi$ -allylic and  $\sigma$  Fe–L bonds are more stable and their geometry is subject to relatively limited changes.

In the mass spectral investigation of **I**, atypically abundant fragmentation was observed in LSIMS experiments, with fragmentation patterns significantly different from those seen in EI. The lability of the entire complex molecule but relative stability of the Fe–L bond were observed.

## 3. Experimental

Complex **I** was obtained according to the method described in Ref. [7]. Macrocyclic cumulene, 1,4,7,10-tetraphenyl-cyclododecahexa-1,2,3,7,8,9-ene (0.43 mmol) and tri-iron dodecacarbonyl (1.20 mmol) in 40 cm<sup>3</sup> of oxygen-free isooctane were refluxed, chromatographed on Kieselgel 60 (Merck) and recrystallized from *n*-hexane, giving air-stable diamagnetic red crystals. From among two isomers  $\alpha$  (42% yield) and  $\beta$  (0.9%) only  $\alpha$  formed well-shaped crystals suitable for X-ray analysis.

### 3.1. X-ray structure determination

A single crystal of **I**, suitable for X-ray diffraction studies, was mounted on a goniometer head of a four-circle P3 (Siemens AG) diffractometer. The crystal class and the orientation matrix were obtained from the least-squares refinement of 35 reflections using graphite-monochromated Mo–K $_{\alpha}$  radiation ( $\lambda = 0.71073$  Å). Intensities were collected in the  $\omega - 2\theta$  mode. A total of 6284 measured intensities were corrected for Lorentz and polarization factors. An analytical absorption correction (Gaussian integration)

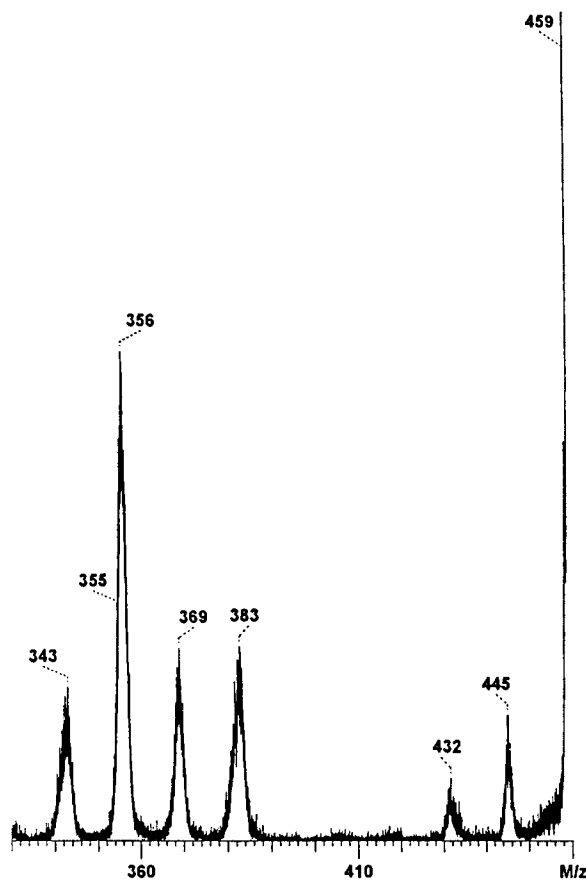


Fig. 5. MIKE spectrum of  $[L]^{+\bullet}$ .

<sup>1</sup> Composition of ions marked by asterisks was not confirmed by accurate mass measurements due to low intensity of signals.

was applied on the basis of the well defined crystals shape.

The structure was solved in  $P\bar{1}$  space group by direct methods using the SHELXS-86 [23] program, which revealed the positions of metal, oxygen and a majority of the C atoms. Full-matrix least-squares refinement method against  $F^2$  values was carried out by using the SHELXL-97 program [24]. All non-hydrogen atoms were refined with anisotropic displacement parameters. The H atoms were refined with fixed geometry, riding on their carrier atoms, with isotropic displacement parameters. Difference Fourier maps, calculated at a late stage of the refinement, showed no significant features. The weighting scheme used was  $w^{-1} = \sigma^2(F_o^2) + (0.0438P)^2 + 0.444P$ , where  $P = 1/3(F_o^2 + 2F_c^2)$ . The selected crystallographic data, the parameters of data collections and refinement procedures are presented in Table 3. Crystallographic data for the structural analysis has been deposited with the Cambridge Crystallographic Data Centre, CCDC no. 120643 for compound I.

### 3.2. Mass spectral analysis

Mass spectra were recorded on an AMD-604 double-focusing spectrometer with BE geometry (AMD Intectra, Germany). A standard EI spectrum was obtained with electron energy 70 eV, acceleration voltage 8 kV and ion source temperature 220°C. Samples were introduced using a direct insertion probe heated, when required, in the range 30–120°C. LSIMS spectra were measured on the same instrument using 10 keV  $\text{Cs}^+$  as a primary ion beam and NBA as a matrix. Accurate mass measurements were carried out at a resolution of 8000 (10% valley definition) at a ionization energy of 70 eV and an acceleration voltage of 8 kV by use of PFK or PFTBA as the references.

During the measurements of the MIKE spectrum four scans were recorded and averaged to improve the mass accuracy and signal-to-noise ratio. The daughter-ion spectrum (linked-scan at constant B/E) in the first field-free region was measured under the conditions described for the MIKE spectrum.

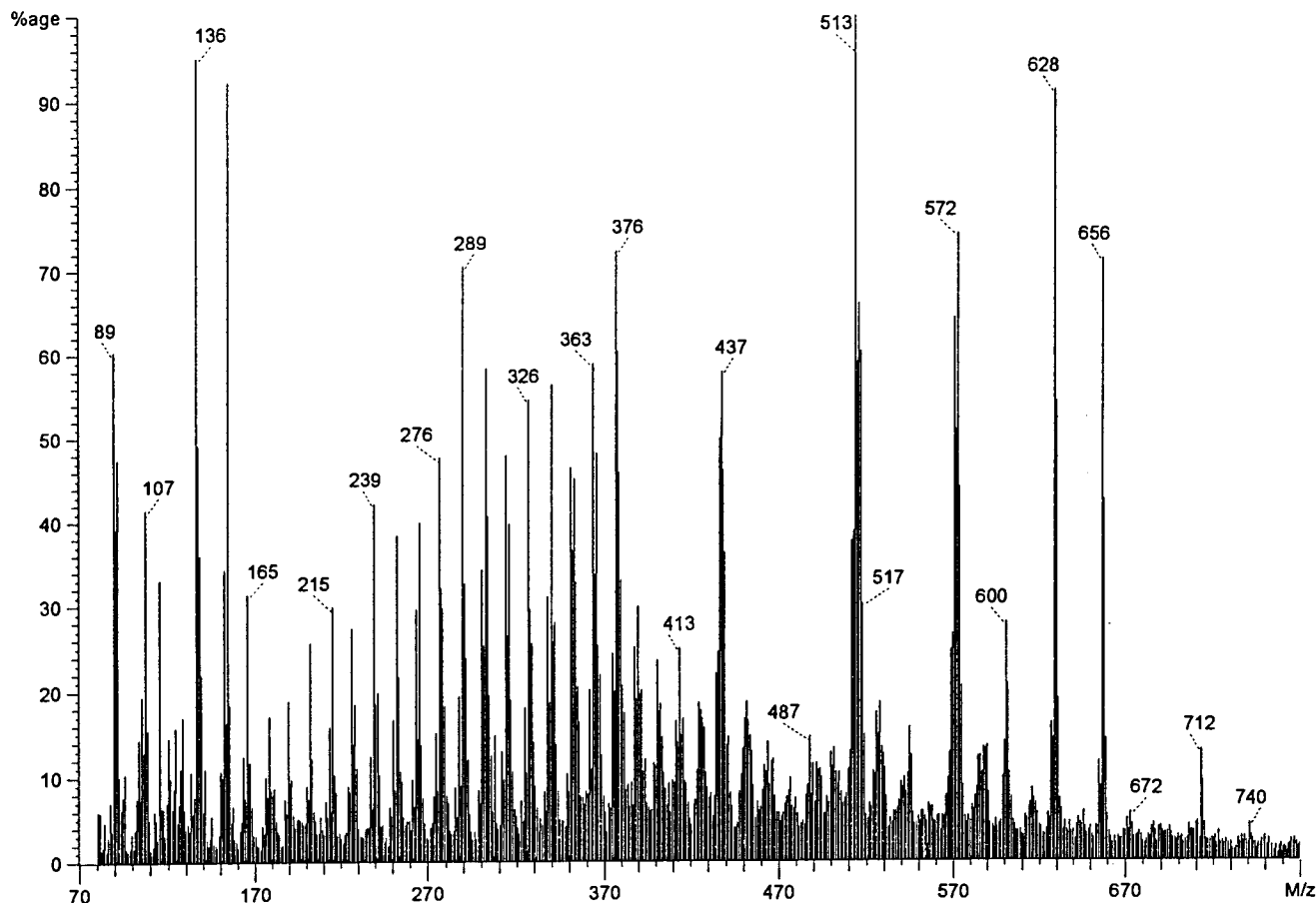


Fig. 6. LSIMS mass spectrum of I.

Table 3  
Crystal data and structure refinement for **I**

Empirical formula	C <sub>42</sub> H <sub>28</sub> Fe <sub>2</sub> O <sub>6</sub>
Formula weight	740.34
Temperature (K)	293(2)
Wavelength (Å)	0.71073
Crystal system	Triclinic
Space group	<i>P</i> $\bar{1}$
<i>a</i> (Å)	11.661(3)
<i>b</i> (Å)	12.733(3)
<i>c</i> (Å)	13.732(3)
$\alpha$ (°)	67.046(17)
$\beta$ (°)	78.382(19)
$\gamma$ (°)	66.139(18)
<i>V</i> (Å <sup>3</sup> )	1714.8(7)
<i>Z</i>	2
<i>D</i> <sub>calc.</sub> (Mg m <sup>-3</sup> )	1.434
Absorption coefficient (mm <sup>-1</sup> )	0.895
<i>F</i> (000)	760
Crystal size (mm <sup>3</sup> )	0.40 × 0.30 × 0.20
$\theta$ range for data collection (°)	2.1–25.0
Index ranges	0 ≤ <i>h</i> ≤ 13, –13 ≤ <i>k</i> ≤ 15, –16 ≤ <i>l</i> ≤ 16
Reflections collected	6284
Independent reflections	5966, <i>R</i> <sub>int</sub> = 0.0144
Completeness to $\theta = 25.0^\circ$	98.2%
Absorption correction	Gaussian, from crystal shape
Max. and min. transmission	0.855 and 0.771
Refinement method	Full-matrix least-squares on <i>F</i> <sup>2</sup>
Data/restraints/parameters	5966/0/482
Goodness-of-fit on <i>F</i> <sup>2</sup>	1.029
Final <i>R</i> indices [ <i>I</i> > 2σ( <i>I</i> )]	<i>R</i> <sub>1</sub> = 0.0325, <i>wR</i> <sub>2</sub> = 0.0792
<i>R</i> indices (all data)	<i>R</i> <sub>1</sub> = 0.0456, <i>wR</i> <sub>2</sub> = 0.0841
Largest difference peak/hole (e Å <sup>-3</sup> )	+0.29/–0.22

## Acknowledgements

We thank Professor Wiesław Jasiobędzki for offering a sample of 1,4,7,10-tetraphenyl-cyclododecahexa-1,2,-3,7,8,9-ene from his collection.

## References

- [1] A. Nakamura, P.J. Kim, N. Hagihara, *J. Organomet. Chem.* 3 (1965) 7.
- [2] K.K. Joshi, *J. Chem. Soc. (A)* (1966) 594.
- [3] D. Bright, O.S. Mills, *J. Chem. Soc. Dalton Trans.* 22 (1972) 2465.
- [4] A. Zimniak, W. Jasiobędzki, *Roczniki Chem.* 49 (1975) 759.
- [5] R. Victor, *J. Organomet. Chem.* 127 (1977) C25.
- [6] S.-E. Eigemann, W. Fortsch, F. Hampel, R. Schobert, *Organometallics* 15 (1996) 1511.
- [7] A. Zimniak, W. Jasiobędzki, *Bull. Acad. Polon. Sci. Ser. Chem.* 23 (1975) 107.
- [8] F.H. Allen, O. Kennard, *Chem. Des. Automat. New.* 8 (1993) 31.
- [9] SACJEL (**1**) is (μ<sub>2</sub>-η<sup>5</sup>,σ<sup>1</sup>-3-ethoxy-3-vinyl-1,2-bis(methoxycarbonyl)allyl)-bis(tricarbonyl-iron). R. Yanez, J. Ros, X. Solans, M. Font-Altaba, R. Mathieu, *New J. Chem. (Nouv. J. Chim.)* 12 (1988) 589.
- [10] KAVPOM (**2**) is (μ<sub>2</sub>-5-*N,N*-(diethylamino)penta-1,3-dien-5-ylidene)-bis(tricarbonyl-iron). E. Cabrera, J.C. Daran, Y. Jeannin, *Organometallics* 8 (1989) 1811.
- [11] HCXOFE (**3**) is hexacarbonyl-(2-4-η<sup>3</sup>,5-6-η<sup>2</sup>-(7-oxo-octa-3,5-diene-2-yl)-di-iron). R. Aumann, H. Averbeck, C. Kruger, *Chem. Ber.* 108 (1975) 3336.
- [12] FOJTED (**4**) is (μ<sub>2</sub>-η<sup>3</sup>,η<sup>2</sup>,σ<sup>1</sup>-5-ethoxy-1,2-bis(trimethylsilyl)-penta-2,4-dienyl)-bis(tricarbonyl-iron). X. Solans, M. Font-Altaba, R. Yanez, J. Ros, R. Mathieu, *Acta Crystallogr. Sect. C (Cr. Str. Commun.)* 43 (1987) 1533.
- [13] CORWEL10 (**5**) is (μ<sub>2</sub>-σ<sup>2</sup>,η<sup>4</sup>-5-methoxy-1,2-bis(trifluoromethyl)-penta-2,4-dien-1-ylidene)-bis(tricarbonyl-iron). J. Ros, G. Comenges, R. Mathieu, X. Solans, M. Font-Altaba, *J. Chem. Soc. Dalton Trans.* (1985) 1087.
- [14] HCPAFE (**6**) is (μ<sub>2</sub>-η<sup>3</sup>,η<sup>2</sup>-1,2,3-triphenylallyl)-bis(tricarbonyl-iron). G. Dettlaf, U. Behrens, E. Weiss, *Chem. Ber.* 111 (1978) 3019.
- [15] JUZLIZ (**7**) is (μ<sub>2</sub>-η<sup>2</sup>,η<sup>2</sup>-3-phenyl-but-2-enylidene)-bis(tricarbonyl-iron). G. Gervasio, E. Sappa, *Organometallics* 12 (1993) 1458.
- [16] KETFEB11 (**8**) is (μ<sub>2</sub>-σ<sup>1</sup>,η<sup>3</sup>,η<sup>2</sup>-diphenylmethylene)-hexacarbonyl-di-iron (neutron study). I. Bkouche-Waksman, J.S. Ricci, Jr., T.F. Koetzle, J. Weichmann, W.A. Herrmann, *Inorg. Chem.* 24 (1985) 1492.
- [17] CEDZIU (**9**) is hexacarbonyl-(μ<sub>2</sub>-1η<sup>2</sup>,2-diphenyl-3-ethoxy-η<sup>3</sup>-η<sup>1</sup>-allyl)-di-iron. J. Ros, R. Mathieu, X. Solans, M. Font-Altaba, *J. Organomet. Chem.* 260 (1984) C40.
- [18] KETFEB (**10**) is (μ<sub>2</sub>-σ<sup>1</sup>,η<sup>3</sup>,η<sup>2</sup>-diphenylmethylene)-hexacarbonyl-di-iron. W.A. Herrmann, J. Gimeno, J. Weichmann, M.L. Ziegler, B. Balbach, *J. Organomet. Chem.* 213 (1981) C26.
- [19] BIFXOD (**11**) is hexacarbonyl-(μ-3-(ethoxycarbonyl)-3-(1,2-η-phenyl)-1,2-diphenyl-η<sup>3</sup>:σ<sup>1</sup>-allyl)-di-iron. J. Klimes, E. Weiss, *Chem. Ber.* 115 (1982) 2606.
- [20] F.A. Cotton, J.M. Troup, *J. Chem. Soc. Dalton Trans.* (1974) 800.
- [21] A. Zimniak, *Pol. J. Chem.* 66 (1992) 1051.
- [22] J. Zachara, A. Zimniak, *Acta Crystallogr. C* 54 (1998) 353.
- [23] G.M. Sheldrick, *Acta Crystallogr. Sect. A* 46 (1990) 467.
- [24] G.M. Sheldrick, *SHELXL-97*, Program for Crystal Structure Refinement, University of Göttingen, Germany, 1997.